

## Origin of quantum chaos for two particles interacting by short-range potentials

M. Van Vessen, Jr., M. C. Santos, Bin Kang Cheng, and M. G. E. da Luz\*

*Departamento de Física, Universidade Federal do Paraná, Caixa Postal 19081, 81531-990 Curitiba-PR, Brazil*

(Received 12 February 2001; published 10 July 2001)

We address the problem of two confined one-dimensional particles of arbitrary masses interacting by general short-range potentials. We study under what conditions quantum chaos emerges for the system by analyzing its spectrum statistics. We show that these conditions are directly connected with a specific feature of the underlying classical dynamics, namely, the ergodicity in the changes of the particles momenta. Quantum mechanically this prevents one from obtaining the exact wave function through the Bethe ansatz. Possible extensions for many-body systems are also discussed.

DOI: 10.1103/PhysRevE.64.026201

PACS number(s): 05.45.-a, 03.65.Ge, 03.65.Db, 03.65.Sq

In general, the emergence of quantum chaos in a single-particle system is a direct consequence of two factors, the spatial geometry and the form of the external potential. For  $N$ -body problems, however, the mutual interactions also play a fundamental role [1]. In this respect we can cite the properties of two- [2] and multielectron atoms [3], chemical reactions [4], quasiparticle dynamics in trapped Bose condensates [5], and fermionic systems [6]. It has also been pointed out that some chaotic features in semiconductor heterostructures and quantum dots are due to the Coulomb potential between the electrons [7].

For a system of many interacting particles, one expects it to be very difficult to determine (i) the exact key mechanisms generating quantum chaos; (ii) how such mechanisms are related to the underlying classical dynamics; and (iii) how to control them through relevant parameters. Needless to say these are not questions of only theoretical interest; they can have practical importance. For instance, chaos can prevent a system being used as a quantum computer [8], so to understand what originates chaos in the system may be fundamental to overcome the problem [9]. A simpler case where the above points may be answered is for  $N=2$ . Indeed, some aspects of quantum chaos in two-particle problems have been analyzed [2,10], but as far as we know, questions (i)–(iii) have not been addressed in the literature.

In this contribution we discuss the problem of two particles that interact through repulsive short-range potentials. From numerical calculations and some analytical results we characterize the situations where quantum chaos occurs. By comparing the quantum with the corresponding classical systems we find a direct connection between the chaotic behavior in the former and a specific feature of the latter: the large number of different momenta the classical particles can have (which is connected to the form of the interaction and the values of some parameters). We argue that this proliferation of different momenta prevents one from obtaining in the quantum case the system wave function by the Bethe ansatz. Finally, we discuss possible implications of our findings for similar many-body problems.

We consider two spinless one-dimensional (1D) particles of masses  $\mu$  and  $\gamma\mu$ , interacting via a potential  $V(|x_1$

$-x_2|)$  which vanishes if the distance between them is greater than  $d/2$ . We shall analyze two different types of confinement for the particles, leading to the boundary conditions  $\Psi(x_1=0 \text{ or } L, x_2)=\Psi(x_1, x_2=0 \text{ or } L)=0$  (box case) and  $\Psi(x_1+L, x_2)=\Psi(x_1, x_2+L)=\Psi(x_1, x_2)$  (torus case). The particles have the wave numbers  $k_1$  and  $k_2$  with  $E=\hbar^2(k_1^2+k_2^2/\gamma)/(2\mu)$ . For  $\gamma=1$  the eigenfunctions of the system are either symmetric or antisymmetric with respect to the interchange  $x_1\leftrightarrow x_2$ , so we have bosons, fermions, or distinguishable particles simply by choosing (or not) a particular symmetry of  $\Psi$ . In all the numerical calculations we will set  $\hbar=\mu=L=1$ .

We start with  $V=\lambda\delta(x_1-x_2)$ . For  $\gamma=1$  the Bethe ansatz provides the exact wave functions for both torus [11] and box [12] cases. For  $\gamma\neq 1$  we numerically solve the Schrödinger equation. From the eigenvalues we calculate the spectrum level spacing distribution  $P(s)$  and the rigidity  $\bar{\Delta}_3(l)$  [13]. We have tested different values of  $\lambda$  and  $\gamma$ . For  $\gamma=1$ , as it should be, the level statistics analysis show characteristics of integrable systems for all cases (for the box case see also [14]). The same is observed for the torus case with  $\gamma\neq 1$ . However, for the box case with  $\gamma\neq 1$  the spectrum statistics can have characteristics of chaotic quantum systems for  $\lambda$  not too small (see the discussion later). A typical result is displayed in Fig. 1 [as is usual, we use only states with the same spatial symmetry to make the level statistics, which here are the states symmetric under  $(x_1, x_2)\leftrightarrow(L-x_1, L-x_2)$ ]. So for a  $\delta$  interaction it seems that  $\gamma\neq 1$  is essential to obtain chaotic behavior. Furthermore, the box type of boundary condition also plays an important role since there is no quantum chaos for the torus case.

We now analyze a general short-range  $V$ . For it we consider the center-of-mass and relative coordinates. In the two-dimensional configuration space  $x_1-x_2$ , the system is restricted to a square region with corners  $(x_1, x_2)$  at  $A=(0,0)$ ,  $B=(L,0)$ ,  $C=(L,L)$ , and  $D=(0,L)$ . For the box case the four sides of this square are infinite walls, whereas for the torus case we have the equivalent sides  $\overline{AB}\equiv\overline{DC}$  and  $\overline{AD}\equiv\overline{BC}$ . We now set  $x=x_1-x_2$ ,  $X=(x_1+\gamma x_2)/(1+\gamma)$ ,  $\mu_{\text{red}}=\mu/(1+\gamma^{-1})$ , and  $\mu_{\text{cm}}=(1+\gamma)\mu$ . The square becomes a rhombus, whose sides are either infinite walls or equivalent two by two as above. The new boundary conditions for the wave functions are  $\Psi|_{\text{walls}}=0$  (box case) and

\*Email address: luz@fisica.ufpr.br

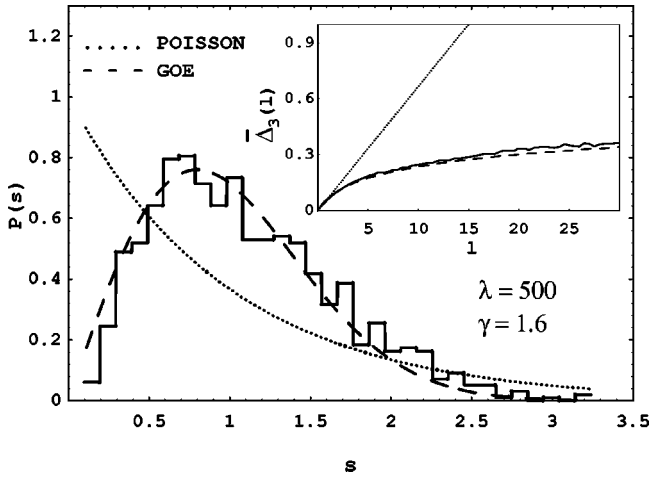


FIG. 1. The level spacing distribution and the rigidity (inset) calculated with the first 1000 levels of a particular spatial symmetry (see text) of the box case with  $\delta$  interaction and  $\gamma \neq 1$ . The dotted and dashed curves represent, respectively, the theoretically expected spectrum statistics for regular and chaotic systems. The numerical results show very good agreement with the GOE predictions.

$\Psi(x, X) = \Psi(x + L, X + L/(1 + \gamma)) = \Psi(x - L, X + \gamma L/(1 + \gamma)) = \Psi(x, X + L)$  (torus case). Defining  $k = (k_1 - k_2/\gamma)/(1 + \gamma^{-1})$  and  $K = k_1 + k_2$  then  $E = \hbar^2 k^2/(2\mu_{\text{red}}) + \hbar^2 K^2/(2\mu_{\text{cm}})$ .

Let us discuss the torus case with  $\gamma = 1$ , for which the boundary conditions simplify to  $\Psi(x, X) = \Psi(x \pm L, X + L/2) = \Psi(x, X + L)$ . This problem can be separated into two one-dimensional systems. To solve them we use a Green's function approach, based on a sum over scattering paths [15], which will be very instructive for our later discussions. Figure 2(a) displays a few examples of what we call vertical (parallel to the  $x$  axis) and horizontal (parallel to the  $X$  axis) orbits. The vertical (horizontal) orbits are composed of two branches, whose total length is always  $2L$  ( $L$ ). If a particle is in one of the branches, say the left, of a given vertical orbit and goes up (down), hitting the side  $\overline{AB}$  ( $\overline{AD}$ ), then it comes out in the corresponding second branch from  $\overline{DC}$  ( $\overline{BC}$ ). Any of these trajectories can be mapped into the one-dimensional systems shown in Fig. 2(b), which differ from each other only by the relative location of the potential  $V$  in the periodic region  $(-L/2, +L/2)$ ; see Fig. 2(c). Thus, they are all equivalent. Similarly, if a particle is in the upper branch of a horizontal orbit and hits the side  $\overline{AB}$  ( $\overline{BC}$ ), it comes out from  $\overline{DC}$  ( $\overline{AD}$ ) in the lower branch. For the horizontal orbits, neither of the two branches is in the region of action of  $V$  (recall that the dynamics of the center of mass is free). All these orbits can be associated with a 1D rigid rotator.

Based on [15] we can write the exact Green's function for the first one-dimensional problem as  $G^\pm(x_f, x_i, k) = \mu_{\text{red}} / (i\hbar^2 k) \sum_{\text{SP}} (\pm 1)^{\theta_{\text{SP}}} W_{\text{SP}} \exp[iS_{\text{SP}}(x_f, x_i; k)/\hbar]$ , where  $x_i$  and  $x_f$  are outside the region of action of the potential. The sum is performed over all the scattering paths (SP's) which are generated by multiple scattering due to the localized  $V$ . Figure 2(b) shows some of these paths schematically. For a given SP, the action  $S_{\text{SP}}$  is  $k$  times the total

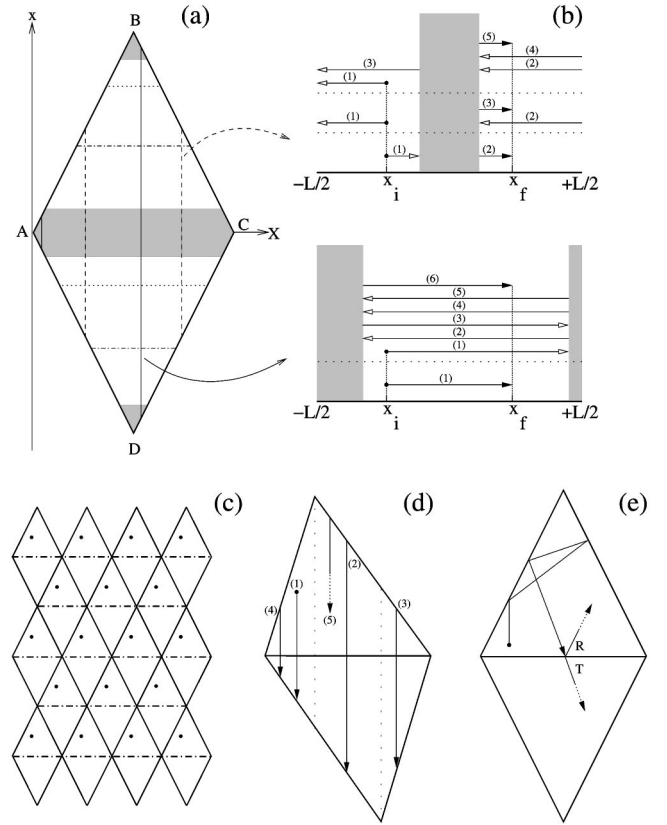


FIG. 2. (a) For the circle case, two vertical and two horizontal representative orbits in the center-of-mass and relative coordinates for  $\gamma = 1$ . The shadows represent the regions of action of the potential. (b) Examples of SP's in the system associated with the vertical orbits. (c) A set of equivalent points (by the wave function boundary conditions) represented in a sequence of replicas of the rhombus region. We see that along  $x$  the periodicity is  $L$ , justifying the periodicity  $L$  of the one-dimensional systems in (b). (d) Some branches of a vertical orbit in the case of  $\gamma \neq 1$  and a  $\delta$  interaction. (e) Part of a raylike trajectory for the box case with  $\gamma = 1$  and a  $\delta$  interaction. Observe that there are no longer independent vertical and horizontal orbits.

length of the particle's trajectory (outside the potential region) and  $W_{\text{SP}}$  is the product of all the usual reflection  $r$  and transmission  $t$  quantum amplitudes that the particle goes through along the scattering path.  $\theta$  is the total number of times that a given trajectory crosses the border at  $-L/2 \equiv +L/2$ . After classifying and summing over all the possible trajectories we find  $(\phi = k(L - d), g^\pm = (1 \mp t \exp[i\phi])^2 - (r \exp[i\phi])^2)$

$$G_{\text{rel}}^\pm(x_f, x_i; k) = \frac{\mu_{\text{red}}}{i\hbar^2 k} \frac{1}{g^\pm} (\mp g^\pm \exp[ik(x_f - x_i + L)] + (\pm 1 - t \exp[i\phi]) \{ \exp[ik(x_f - x_i + L)] + \exp[-ik(x_f - x_i + L)] \} \pm r \exp[i\phi] \times \{ \exp[ik(x_f + x_i)] + \exp[-ik(x_f + x_i)] \}).$$

For the rigid-rotator-like problem the Green's function is

$G_{\text{cm}}(X_f, X_i; K) = (\mu_{\text{cm}} / i\hbar^2 K) \{ \exp[iK|X_f - X_i|] + \exp[iK(L - |X_f - X_i|)] \} / w$ , with  $w = 1 - \exp[iKL]$ .

The energy eigenvalues are obtained from the poles of the Green's functions, which are given by the roots of  $(t \pm r) \exp[ik(L-d)] = 1$  for  $G_{\text{rel}}^+$ ,  $(t \pm r) \exp[ik(L-d)] = -1$  for  $G_{\text{rel}}^-$ , and  $KL = 2n\pi$  (with  $n$  being an integer) for  $G_{\text{cm}}$ . Since for separable systems the total energy is just the sum of the energies of each degree of freedom, we can write  $E = E_{\text{rel}} + E_{\text{cm}}$ . By calculating the residues of the Green's functions at the energy eigenvalues one obtains  $\psi_{\text{rel}}(x)$  and  $\psi_{\text{cm}}(X)$ , and thus  $\Psi(x, X) = \psi_{\text{rel}}(x) \psi_{\text{cm}}(X)$ . Here, however, some care is in order due to the particular form of the boundary condition imposed on  $\Psi$ . In fact, the total wave function must obey  $\psi_{\text{rel}}(x) \psi_{\text{cm}}(X) = \psi_{\text{rel}}(x+L) \psi_{\text{cm}}(X+L/2)$ . It is easy to see that  $\psi_{\text{rel}}^{\pm}$  (coming from  $G_{\text{rel}}^{\pm}$ ) is such that  $\psi_{\text{rel}}^{\pm}(x+L) = \pm \psi_{\text{rel}}^{\pm}(x)$ . Furthermore,  $\psi_{\text{cm}}^{(n)}(X+L/2) = (-1)^n \psi_{\text{cm}}^{(n)}(X)$ . Therefore,  $\Psi$  must be written either as  $\psi_{\text{rel}}^+ \psi_{\text{cm}}^{(n=\text{even})}$  with energies  $E = E_{\text{rel}}^+ + E_{\text{cm}}^{n=\text{even}}$  or as  $\psi_{\text{rel}}^- \psi_{\text{cm}}^{(n=\text{odd})}$ , with  $E = E_{\text{rel}}^- + E_{\text{cm}}^{n=\text{odd}}$ . These results give us the exact solution for the torus case with  $\gamma=1$  and a general short-range potential  $V$ .

To verify the above expressions we have considered the case of a  $\delta$ -function potential, where  $d=0$ ,  $t_{\delta} = ik/(ik - \sigma)$ ,  $r_{\delta} = \sigma/(ik - \sigma)$ , and  $\sigma = \mu_{\text{cm}} \lambda / \hbar^2$ . After simple calculations we obtained all the exact solutions previously derived in the literature [11]. We have also considered other types of  $V$ , for instance, rectangular and triangular barriers. We computed the eigenenergies with these potentials numerically and compared them with the energies obtained from our solution; we found a perfect agreement, as it should be.

For the torus case with  $\gamma \neq 1$ , in general the vertical orbits do not all have the same total length and do not close perfectly [see Fig. 2(d)]. However, we can still solve this case exactly. Here we just write down the equations that give the correct eigenvalues (details will appear elsewhere [16]),  $\exp[i(k_1 + k_2)L] = 1$  and  $(t - \exp[ik_2L])(t - \exp[i\{(1-\gamma)k_1 + 2k_2\}L/(1+\gamma)]) = r^2$ , which reduce to our previous formulas for  $\gamma=1$ .

The box case is not separable into the center-of-mass and relative coordinates [see Fig. 2(e)], but can still be solved by the Bethe ansatz for  $\gamma=1$  and a  $\delta$  interaction [12]. To analyze this same problem but for a short-range  $V$  we have numerically calculated the spectrum considering a rectangular barrier, i.e.,  $V = V_0$  for  $|x_1 - x_2| < d/2$  and zero otherwise. An example of the level statistics for bosons is shown in Fig. 3, indicating chaotic behavior (fermions present similar level statistics). These results are not at all a surprise because this system is equivalent to a two-dimensional billiard problem [17], where the particle experiences different potentials in different regions of the billiard. In fact, it has been implemented experimentally by microwave cavities loaded with a different dielectric medium [18] and shows the so called phenomenon of ray splitting, much studied in the context of quantum chaos [19].

At this point it is worth summarizing our findings so far. For the torus case, regardless of the value of  $\gamma$  and the form of the interaction, we never see quantum chaos. For the box case and a  $\delta$  interaction, we have that for  $\gamma=1$  the system is

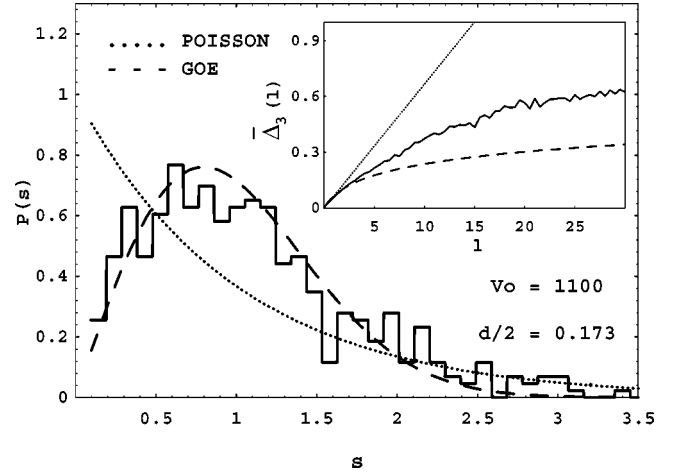


FIG. 3. The same plots as in Fig. 1, but now for the box case with a rectangular barrier interaction and  $\gamma=1$ . The spectrum statistics are made with the first 450 energy levels of the eigenstates symmetric under both  $x_1 \leftrightarrow x_2$  (bosons) and  $(x_1, x_2) \leftrightarrow (L - x_2, L - x_1)$ . Here we also see a fair agreement with the GOE predictions.

regular and for  $\gamma \neq 1$  it can present chaos (Fig. 1). Moreover, for a general short-range potential  $V$ , e.g., a rectangular barrier, the box case may have chaotic spectrum statistics even for  $\gamma=1$ .

In order to seek a connection between all the above results and the corresponding classical dynamics we turn to the classical system of two impenetrable particles in 1D which has been analyzed in different aspects such as ergodicity, mixing, distributions of momenta transfer, etc. [20]. Here we just list some results that are important for our purposes. If the classical particles interact only via elastic collisions, we have the relation between the momenta before and after the collision by simple laws of conservation. Furthermore, the confinement of the particles, within a circle (in the torus case) or inside a box, gives rise to infinitely many collisions, leading to a whole set of different  $p$ 's for them. Thus, we have the following [20]. For the torus case, (i) the particles recover their initial momenta after two successive collisions for any value of  $\gamma$ . For the box case, (ii) when  $\gamma=1$  the particle-particle and the wall-particle collisions lead to  $p_1^{(a)} = p_2^{(b)}$ ,  $p_2^{(a)} = p_1^{(b)}$ , and  $p_j^{(a)} = -p_j^{(b)}$ , so in total each particle can assume only four different values of momentum. For  $\gamma \neq 1$  and  $\eta = \theta/\pi$  ( $\cos[\theta] = (1-\gamma)/(1+\gamma)$ ), (iii) for rational  $\eta$  just a finite set of distinct momentum pairs  $(p_1, p_2)$  can occur and, (iv) for irrational  $\eta$ , although all the possible  $(p_1, p_2)$  are generated very slowly [20], they can assume infinitely many different values.

If the particles interact by a short-range  $V$  and scatter elastically we have that (v) in both torus (any  $\gamma$ ) and box ( $\gamma \neq 1$ ) cases the results are similar to (i) and (iv). For the box case with  $\gamma=1$ , (vi) contrary to (ii), proliferation of  $p$ 's can occur. To see this consider as interaction a rectangular barrier (see above) and initially particles with kinetic energies greater than  $V_0$ . Assume the particles are less than  $d/2$  apart and close to the right wall, going toward it. If particle 1 collides with the wall first, reverses its motion, and then hits particle 2, simple calculations show that when their distance

apart is greater than  $d/2$  their momenta will not be given simply by an exchange as in (ii). Both particles will have new momenta values, resembling what happens in the case of  $\gamma \neq 1$ . Repetitions of this process, which depends on  $d/L$ , then generate a large set of different  $p$ 's.

By putting all the previous results together we can establish a *direct correspondence* between the origin of chaos in the quantum case and the ergodicity of the momenta in the classical case. In fact, we see that when classically the system has a finite (infinite) number of possible values for the  $p$ 's the quantum system is always regular (chaotic). To understand the origin of this correspondence let us consider the scattering wave function of two particles interacting by a general short-range potential. If particle 1 is initially on the left of particle 2, we have (symmetrization considerations for boson and fermions, when  $\gamma=1$ , are not relevant here)

$$\begin{aligned} \psi(x_2 - x_1 > d/2) = (2\pi)^{-1} \{ & \exp[i(k_1^{(b)}x_1 + k_2^{(b)}x_2)] \\ & + r(k) \exp[i(k_1^{(a)}x_1 + k_2^{(a)}x_2)] \}, \end{aligned}$$

$$\psi(x_1 - x_2 > d/2) = (2\pi)^{-1} t(k) \exp[i(k_1^{(b)}x_1 + k_2^{(b)}x_2)],$$

with  $k_1^{(a)} = [(1-\gamma)/(1+\gamma)]k_1^{(b)} + [2/(1+\gamma)]k_2^{(b)}$  and  $k_2^{(a)} = [(\gamma-1)/(1+\gamma)]k_2^{(b)} + [2\gamma/(1+\gamma)]k_1^{(b)}$ . It is easy to see that these relations between the  $k$ 's are exactly the ones for the exchange of momenta in a collision of two classical impenetrable particles (recall that  $p = \hbar k$ ). Thus, when the quantum particles tunnel through (reflect from) each other, with probability  $|t(k)|^2$  ( $|r(k)|^2$ ), they do not change (change exactly as in the classical case) their momenta. By confining our quantum system, its eigenstates  $\Psi$  can be expressed as the superposition of all these scattering solutions [21], analogous to our construction for the Green's function, written as a sum over scattering paths. In this sense, the proliferation of momenta in the classical system does also occur in the quantum case. Here it also becomes clear why  $\lambda$  (or  $V_0$  in the case of a rectangular barrier interaction) cannot be too small for the system to be chaotic. This is because the exchange of momenta in the quantum case takes place only in the reflections, which occur with probability  $|r|^2$ , thus being small for  $\lambda$  small.

For  $N$  identical particles with pairwise interactions, we have the following. (a) For  $\delta$  potentials the Bethe ansatz (BA) leads to  $\Psi(x_1, \dots, x_N) = \sum_P \mathcal{C}(P) \exp[i \sum k_p x_i]$ , where the sum runs over all the permutations of the initial set  $\{k_1, \dots, k_N\}$ . The  $\mathcal{C}(P)$ 's take care of both the form of the interactions and the correct symmetries of the wave function. (b) For long-range decaying potentials, Sutherland (see, for instance, [22] and references therein) introduced the asymptotic BA, applied when the many-body  $S$  matrix can be decomposed into two-body matrices in the asymptotic region  $x_1 \ll x_2 \ll x_3 \dots$ . (c) For short-range  $V$ 's this decomposition occurs in the regions outside the actions of the potential and the Schrödinger equation has as solution a linear combination of plane waves. So the asymptotic BA method does give the exact  $\Psi$  in such regions. In our torus case (short-range  $V$ , any  $\gamma$ ) we have [16]  $\Psi = \mathcal{A}(r(k),$

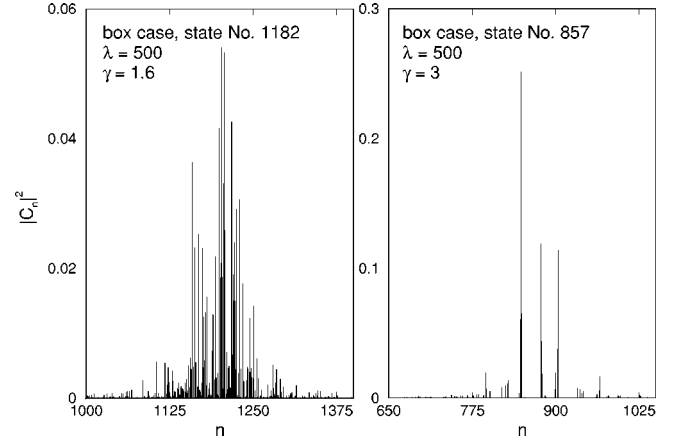


FIG. 4. Typical  $c_n$  distributions for chaotic ( $\gamma=1.6$ ) and regular ( $\gamma=3$ )  $\Psi$ 's. Here the two states have their energies differing by only 0.1%.

$t(k) \exp[i(k_1^{(b)}x_1 + k_2^{(b)}x_2)] + \mathcal{B}(r(k), t(k)) \exp[i(k_1^{(a)}x_1 + k_2^{(a)}x_2)]$ , valid for  $d/2 < x_1 - x_2 < L$ , and a similar expression for  $d/2 < x_2 - x_1 < L$ . The  $k_j$ 's in the exponentials are not just permutations of the initial set of momenta, they also include all the new  $k_j$ 's generated by the collisions.  $\mathcal{A}$  and  $\mathcal{B}$  depend explicitly on the transmission and reflection amplitudes for  $V$  [16]. This exact wave function is then a generalization of the BA to our case. Extending this idea we should write  $\Psi$  for the box case (in the ergodic regime) as a sum over an infinite set of  $k$ 's due to the ‘‘quantum proliferation’’ of momenta discussed above. Thus we cannot have  $\Psi$  in a closed form and the system must present chaotic features as a consequence of the Berry hypothesis [23], which states that the wave function of a chaotic system has the same statistical properties as a sum of random waves. In our case,  $\Psi$  is written as a random sum of an infinite number of plane waves, where the randomness is caused by the ergodicity in the  $p$ 's.

A very simple way to verify the above ideas is to write the system state  $m$  as  $\Psi_m = \sum_n c_{mn} \phi_n$ , where  $\phi_n$  are the eigenstates of two noninteracting confined particles (which for the box case are sine functions), with  $n \equiv (n_1, n_2)$  the momentum quantum numbers (in order of increasing energy). From the previous discussions one would expect to have a much broader distribution of  $c_n$ 's for a chaotic than for an integrable case. The spread of momenta due to the successive collisions implies a much larger number of unperturbed eigenstates necessary to describe  $\Psi$  accurately. We have tested this for a large number of cases and a typical situation is shown in Fig. 4. For the box case with a  $\delta$  interaction we compare the  $|c_n|^2$  distribution for  $\gamma=1.6$  (see Fig. 1) with  $\gamma=3$ , which is regular (the number of different momenta the particles can have in this case is finite [20]). To have a criterion when comparing different systems we have chosen the state quantum numbers  $m$  in such a way that their energy values are very close. We should mention that for a chaotic system the  $c_n$ 's are more or less distributed depending on  $m$ . But their distribution is always much broader than those of a regular case.

Based on all the above results we conjecture that for  $N$  confined particles of arbitrary masses and interacting pair-

wise by short-range potentials  $V_{ij}$ , the total  $\Psi$  outside the regions of interaction is a linear combination of plane waves whose coefficients are related to the quantum  $r_{ij}$ 's and  $t_{ij}$ 's, and the  $k$ 's in the exponentials are the same as the ones generated by collisions in the classical case. Obviously, we can obtain  $\Psi$  in a closed form only if the total number of  $k$ 's is finite. Thus one can affirm that for  $N \geq 3$  both the torus and the box cases present quantum chaos (except for some values of  $\gamma$ ) since classically they are ergodic [20].

We finally mention that some of our results can be interpreted in terms of analogies with triangular and rhombus billiards [24]. However, those analogies do not work in all cases, as will be the subject of a future contribution (see also [17]).

Valuable help from J. A. Freire and C. Carvalho is acknowledged. Partial financial support for this work was provided by CNPq and PADCT (Proj. No. 620081/97-0).

- 
- [1] V. Zelevinsky, *Int. J. Mod. Phys. B* **13**, 569 (1999).  
 [2] D. Wintgen, K. Richter, and G. Tanner, *Chaos* **2**, 823 (1992); D. Wintgen, A. Burgers, K. Richter, and G. Tanner, *Prog. Theor. Phys. Suppl.* **116**, 121 (1994).  
 [3] V. V. Flambaum, A. A. Gribakina, G. F. Gribakin, and I. V. Ponomarev, *Physica D* **131**, 205 (1999).  
 [4] G. Grossi, L. Peroncelli, and N. Rahman, *Chem. Phys. Lett.* **313**, 639 (1999).  
 [5] M. Fliesser and R. Graham, *Physica D* **131**, 141 (1999); M. Fliesser, A. Csordas, R. Graham, and P. Szepfalusy, *Phys. Rev. A* **56**, 4879 (1997).  
 [6] B. D. Simons, P. A. Lee, and B. L. Altshuler, *Phys. Rev. Lett.* **72**, 64 (1994); R. Melin, *J. Phys. I* **5**, 787 (1995); V. V. Flambaum and F. M. Izrailev, *Phys. Rev. E* **55**, R13 (1997); P. Jacquod and D. L. Shepelyansky, *Phys. Rev. Lett.* **79**, 1837 (1997); B. Georgeot and D. L. Shepelyansky, *ibid.* **79**, 4365 (1997).  
 [7] C. M. Marcus *et al.*, *Chaos, Solitons Fractals* **8**, 1261 (1997); S. E. Ulloa and D. Pfannkuche, *Superlattices Microstruct.* **21**, 21 (1997); D. Ullmo, H. U. Baranger, K. Richter, F. von Oppen, and R. A. Jalabert, *Phys. Rev. Lett.* **80**, 895 (1998).  
 [8] V. V. Flambaum, *Aust. J. Phys.* **53**, 489 (2000); B. Georgeot and D. L. Shepelyansky, *Phys. Rev. E* **62**, 3504 (2000).  
 [9] B. Georgeot and D. L. Shepelyansky, *Phys. Rev. E* **62**, 6366 (2000).  
 [10] K. Patel, M. S. Desai, V. Potbhare, and V. K. B. Kota, *Phys. Lett. A* **275**, 329 (2000); L. Kaplan and T. Papenbrock, *Phys. Rev. Lett.* **84**, 4553 (2000); X. Waintal, D. Weinmann, and J. L. Pichard, *Eur. Phys. J. B* **7**, 451 (1999); L. Meza-Montes and S. E. Ulloa, *Physica B* **251**, 224 (1998); F. Borgonovi, I. Guarneri, F. M. Izrailev, and G. Casati, *Phys. Lett. A* **247**, 140 (1998); T. Cheon and T. Shigehara, *ibid.* **233**, 11 (1997); F. Borgonovi and D. L. Shepelyansky, *Nonlinearity* **8**, 877 (1995).  
 [11] E. H. Lieb and W. Liniger, *Phys. Rev.* **130**, 1605 (1963); J. B. McGuire, *J. Math. Phys.* **6**, 432 (1965).  
 [12] M. Gaudin, *Phys. Rev. A* **4**, 386 (1971).  
 [13] M. C. Gutzwiller, *Chaos in Classical and Quantum Physics* (Springer, New York, 1990).  
 [14] C. H. Lewenkopf, *Phys. Rev. A* **42**, 2431 (1990).  
 [15] M. G. E. da Luz, E. J. Heller, and B. K. Cheng, *J. Phys. A* **31**, 2975 (1998).  
 [16] M. G. E. da Luz *et al.* (unpublished).  
 [17] G. Manfredi, J. L. Rouet, and R. Dufour, *Eur. J. Phys.* **14**, 206 (1993).  
 [18] S. Bauch, A. Bledowski, L. Sirko, P. M. Koch, and R. Blümel, *Phys. Rev. E* **57**, 304 (1998).  
 [19] L. Couchman, E. Ott, and T. M. Antonsen, Jr., *Phys. Rev. A* **46**, 6193 (1992).  
 [20] G. Casati and J. Ford, *J. Comput. Phys.* **20**, 97 (1976); J. L. Rouet, F. Blasco, and M. R. Feix, *J. Stat. Phys.* **71**, 209 (1993); M. Hasegawa, *Phys. Lett. A* **242**, 19 (1998).  
 [21] M. G. E. da Luz, A. S. Lupu-Sax, and E. J. Heller, *Phys. Rev. E* **56**, 2496 (1997).  
 [22] B. Sutherland, *Phys. Rev. Lett.* **75**, 1248 (1995).  
 [23] M. V. Berry, *J. Phys. A* **10**, 2083 (1977).  
 [24] A. G. Miltenburg and Th. W. Ruijgrok, *Physica A* **210**, 476 (1994); G. Casati and T. Prosen, *Phys. Rev. Lett.* **83**, 4729 (1999); D. Biswas and S. R. Jain, *Phys. Rev. A* **42**, 3170 (1990).